

Transport in Hamiltonian systems with slowly changing phase space structure

Freddy Bouchet¹ and Eric Woillez^{1,2*}

1) Univ Lyon, Ens de Lyon, Univ Claude Bernard, CNRS, Laboratoire de Physique, F-69342 Lyon, France.

2) Department of Physics, Technion, Haifa 32000, Israel.

Keywords: Hamiltonian chaos, averaging, long time transport, rare events.

Abstract

Transport in Hamiltonian systems with weak chaotic perturbations has been much studied in the past. In this paper, we introduce a new class of problems: transport in Hamiltonian systems with slowly changing phase space structure that are not order one perturbations of a given Hamiltonian. This class of problems is very important for many applications, for instance in celestial mechanics. As an example, we study a class of one-dimensional Hamiltonians that depend explicitly on time and on stochastic external parameters. The variations of the external parameters are responsible for a distortion of the phase space structures: chaotic, weakly chaotic and regular sets change with time. We show that theoretical predictions of transport rates can be made in the limit where the variations of the stochastic parameters are very slow compared to the Hamiltonian dynamics. Exact asymptotic results can be obtained in the classical case where the Hamiltonian dynamics is integrable for fixed values of the parameters. For the more interesting chaotic Hamiltonian dynamics case, we show that two mechanisms contribute to the transport. For some range of the parameter variations, one mechanism -called "transport by migration with the mixing regions" - is dominant. We are then able to model transport in phase space by a Markov model, the local diffusion model, and to give reasonably good transport estimates.

1 Introduction

Transport in Hamiltonian systems and is a classical field of dynamical system theory [1, 2, 3, 4], with a huge number of applications [5, 6]. Beyond deterministic dynamical systems, a lot of work has been devoted in the past to study the effect of random perturbations [7], more specifically on Hamiltonian systems and on area preserving maps, for instance in the context of plasma physics [8, 9]. Noise is always present in real natural systems and in experiments because of the effect of hidden chaotic degrees of freedom. Even of small amplitude, noise plays a very important role in the long term behavior of the dynamics, and on transport properties. One usually models the hidden degrees of freedom by an additional stochastic process of small amplitude acting on the system. For example, the effect of noise on the standard map or on other classical area preserving maps has been studied earlier in [10, 11, 2], motivated by the dynamics of charged particles in accelerators. More recently, with the development of stochastic calculus, [12, 13] have studied the generic effect of small stochastic perturbations of Hamiltonian flows, and [14, 15] have derived a diffusion equation for the slow action variable in Hamiltonian systems. In particular, [12, 13] have rigorously justified the averaging principle in Hamiltonian systems and studied the slow diffusive motion of action variables. The important point is that all those works fall in the dynamical framework

$$\dot{x} = \frac{1}{\epsilon} F(x) + \beta \left(x, \frac{t}{\epsilon} \right), \quad (1)$$

where F is a Hamiltonian vector field, β is a deterministic or a stochastic perturbation of the Hamiltonian vector field, and ϵ is a small parameter. Qualitatively, we can describe the dynamics of (1) saying that it follows the regular or chaotic orbits of the unperturbed dynamics $\dot{x} = F(x)$ on a fast timescale $\propto \epsilon$, and deviates slowly from those orbits because of the effect of the perturbation β , acting on a timescale of order one. We note that the case (1) where F is a Hamiltonian dynamics and β is a wave of slow modulated frequency has been studied in [16, 17, 18, 19] and can lead to interesting phenomena such as autoresonant motion and acceleration of particles.

*Corresponding author. *Email address:* eric.woillez@technion.ac.il

In this paper, we consider a different framework, which cannot be reduced to the much-studied model (1), and still is essential for many applications. We study a one-dimensional Hamiltonian dynamics which Hamiltonian depends on a slow parameter¹

$$\dot{x} = \frac{1}{\epsilon} J \nabla H(x, \nu(t)), \quad (2)$$

where $x := (p, q)$ represents the vector of canonical variables, and $J := \begin{bmatrix} 0 & -1 \\ 1 & 0 \end{bmatrix}$.

This model has received relatively little attention in the literature compared to Eq. (1), but some nontrivial features have already been emphasized in [20, 21] such as the existence of trajectories with unbounded energy growth. Generally the dynamics (1) can be very different from the dynamics (2) because the variations of ν in Hamiltonian (2) can range over a region of order one. The amplitude of the variations of ν can thus be of the same order as the variations of action variables. We call ν a "slow variable", because one has to wait for a time Δt of order one to observe a variation $\Delta \nu$ of order one, whereas canonical variables have large variations on a timescale $\propto \epsilon$. For any fixed value of the parameter ν , for the Hamiltonian $H(x, \nu)$, the dynamics in its phase space is characterized by strongly chaotic regions, weakly chaotic regions, and in some cases, KAM tori. We call phase space structure the geometry and topology of these chaotic, weakly chaotic, and regular areas. When the parameter ν slowly evolves with time, the geometry and topology of those regions are slowly distorted, and can be dramatically changed for large variations of ν that occur on long times. As a consequence of the distortion of the phase space structure, some regions that might not have been accessible for the system at the initial value of ν become easily accessible when ν changes. This affects drastically the transport in phase space. Let us consider a simple example to illustrate such a change in phase space structure. We take the one and a half degree of freedom Hamiltonian²

$$H(p, q, \Lambda, \lambda, \nu) = \frac{p^2}{2} + \cos(q) + \cos(q - \lambda) + \nu\Lambda, \quad (3)$$

where ν is the frequency of the angle λ and plays the role of the external parameter and is the conjugated angle to Λ . In the Hamiltonian (3), a resonance is defined as the value of p for which one of the two angles q or $q + \lambda$ has zero frequency. We have plotted in figure (1) a snapshot of the phase space structure (p, q) for the Hamiltonian (3) for three different values of ν . The frequency ν is decreasing from the left picture to the right picture. The Poincaré section described by (3) displays two major libration regions, one centered at $p = 0$, and one centered at $p = \nu$. A libration region is defined as a region of phase space where the canonical angle q has bounded oscillations between two extremal values in $[0, 2\pi]$. The libration regions can be very easily recognized on the Poincaré section of figure (1) as they look like "cat's eyes" surrounding the fixed points of resonances. The Hamiltonian flow is only very weakly chaotic in the initial state because the two main resonances are far away from each other, but it becomes more and more chaotic as the two main resonances become closer (for a precise description of such systems, see [2]). The red curves in figure (1) are particular trajectories that start inside the upper libration region. For large enough values of ν , the trajectories are trapped inside the upper libration region (first and second panel of figure (1)). On the contrary, when ν is lower than some critical value, the trajectory can freely transit from one cat's eye to the other (third panel of figure (1)). Imagine now that the frequency ν in Hamiltonian (3) is no longer fixed, but slowly depends on time. Consider then the Hamiltonian

$$H(p, q, \Lambda, \lambda, \nu(t)) = \frac{p^2}{2} + \cos(q) + \cos(q - \lambda) + \nu(t)\Lambda. \quad (4)$$

The three pictures of figure (1) represent instantaneous snapshots of the phase space of the Hamiltonian (4) at three different times. The upper cat's eye centered at $p = \nu$ moves according to the variations of $\nu(t)$. Some trajectories that were trapped in the upper libration region in the initial state can be carried downward by the displacement of the upper libration region and finally reach the lower libration region.

The aim of the example of figure (1) is to show that the slow changes in phase space structure create a particular transport mechanism that is very different from the transport created by small perturbation as in system (1). In the present paper, we investigate the case (2) where the parameter ν is *stochastic*. In particular, we consider in the present work the possibility of strongly irregular functions $\nu(t)$, as happens for example when ν is a diffusion process. This irregularity can be seen, for example, as the result of the influence of chaotic external degrees of freedom that evolve on a timescale much shorter than any other timescale in the Hamiltonian system. We show

¹Note that we could have defined a new Hamiltonian $H' = H/\epsilon$ such that Eq. (2) are indeed Hamilton's equations with H' , but we believe the presentation chosen in this paper emphasizes more clearly the timescale separation in the dynamics.

²Note that we call this model one and a half degree of freedom Hamiltonian because Λ do not play any role in the dynamics.

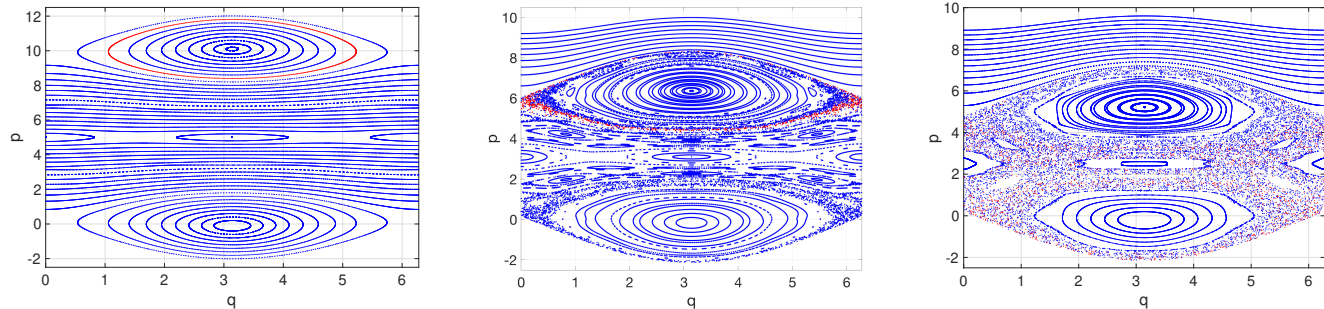


Figure 1: Snapshots of the phase space structure of the Hamiltonian (3) for three different values of ν . The blue curves represent a Poincaré section of the Hamiltonian flow (3). The position of the lower resonance is fixed, but the upper resonance is centered at the value $p = \nu$. Left panel: $\nu \approx 10$, the two main resonances are far away from each other and the phase space is very weakly chaotic. The red trajectory is trapped in the upper libration region. Middle panel: $\nu \approx 6.2$, and chaotic regions become larger in the vicinity of hyperbolic fixed points. The red trajectory is in a chaotic region, but it cannot be carried to the lower libration region because of remaining KAM tori. Right panel: $\nu \approx 5$ and the two main cat's eyes are now connected through a strongly chaotic region. KAM tori have been destroyed and the red trajectory can freely do the transition from one libration region to the other.

that transport in phase space is the result of two mechanisms. We call the first mechanism *noise driven transport in regular regions*. This transport mechanism comes from the strong irregularity of the stochastic trajectories $\nu(t)$, and would not be observed for infinitely differentiable functions $\nu(t)$. We call the second mechanism *transport by slow deformation of chaotic regions*. This second transport mechanism occurs when trajectories are trapped in chaotic regions and follow their displacement to access to other parts of phase space. During the displacement, the extension of the chaotic layer can also vary such that transport is due to both *migration* and *extension* of chaotic regions, as happens for example in Fig. (1). For the generic dynamics (2) both mechanisms, noise driven transport in regular regions and transport by slow deformation of chaotic regions, are present and contribute to transport. Our aim is to separately describe and quantify transport due to the one and the other mechanisms.

All over the paper, we thus consider the Hamilton's equations (2). We first consider in section 2 the case of a one-degree of freedom Hamiltonian of the form $H(p, q, \nu(t))$, which has an integrable dynamics for any fixed value of ν . If the parameter ν would be a regular function of time, transport would be described by the classical theory of adiabatic invariants [22, 23]. For a *stochastic* parameter ν with irregular trajectories, we show that the transport is completely due to the mechanism of noise driven transport in regular regions, and we give a stochastic differential equation to describe the diffusion of adiabatic invariants in the limit $\epsilon \rightarrow 0$, when there is no separatrix crossing during the diffusion process. This result is obtained using standard averaging techniques. We also illustrate our results with the example of the harmonic oscillator. We note that the case of diffusion across a separatrix is much more technical. It has been shown in case of a dynamics of type (1) with separatrix crossing that the motion of the slow variable is given by a diffusion process on a graph where the branches represent the different domains in phase space defined by the separatrix [13]. The change in the value of the adiabatic invariant during separatrix crossing has also been known for a long time [24, 25], and the result could in principle be used to extend our theory also to separatrix crossing for Hamiltonians with one degree of freedom. We do not treat this problem in the present paper as we have chosen to rather deal with the chaotic case where resonances overlap.

The second part 3 of the paper is probably the most original and interesting one. We deal with the much more difficult case where the Hamiltonian dynamics (2) has more than one degree of freedom and is thus chaotic even for fixed values of ν . For simplicity, we study a dynamical system where the width of chaotic regions is almost constant and the deformation only comes from migration of the regions. Our approach could be used in the general case without further difficulties. We show that both transport mechanisms, "noise driven transport in regular regions" and "transport by slow migration of chaotic regions", take place. We explain that the second mechanism is dominant for some range of parameters. The transport can then be reduced to a fully Markovian process in the limit $\epsilon \rightarrow 0$. We call this process the *instantaneous local diffusion model*, because it consists in modeling the chaotic regions of phase space by diffusive regions with infinite diffusion coefficient. We check numerically that the Markov model gives reasonably good estimation of transport rates when the mechanism of transport by slow migration of chaotic regions is dominant.

Our results are relevant in celestial mechanics to study the long term dynamics of the spin axis of planets, and

the secular dynamics of Mercury. Some times ago [26] already pointed out that the dynamics of the obliquity of Mars could be reduced to a model of a pendulum with slowly varying parameters. He used the theory of adiabatic invariants to estimate the probability of Mars to enter into libration. However, this model still considered that the parameters are regular functions of time. With the work of [27, 28], it has been shown that the solar system is chaotic on a timescale of few million years. The set of fundamental frequencies of the Laplace–Lagrange solution, that plays the role of parameters in the Hamiltonian describing the dynamics of spin axes of planets, has thus a stochastic long-term evolution [29]. This justifies the relevance of a model such as (2). This paper was thought of as a theoretical work to put in a general framework the ideas developed in [30] to study the long term dynamics of the Earth obliquity.

2 The integrable case

2.1 Formulation of the model and theoretical results

In this section, we consider a one-degree of freedom Hamiltonian $H(p, q, \nu)$ and Hamilton's equations (2), which are explicitly

$$\begin{cases} \dot{p} &= -\frac{1}{\epsilon} \frac{\partial H}{\partial q}(p, q, \nu(t)) \\ \dot{q} &= \frac{1}{\epsilon} \frac{\partial H}{\partial p}(p, q, \nu(t)) \end{cases} \quad (5)$$

The set (p, q) is the set of canonical variables, and $\epsilon \ll 1$. ν is an external parameter in the Hamiltonian. For any fixed value of the parameter ν , the Hamiltonian has one degree of freedom, and its dynamics is thus integrable. When the parameter ν is a regular, slowly varying function of time, the slow action dynamics is described by the old theory of adiabatic invariants. Even when transport occurs through separatrix crossing, the theory of adiabatic invariants can be extended to account for the discontinuity in the action definition (see [24, 25] and [31] for a review).

We consider here a case where the parameter ν is stochastic, and we assume that no separatrix crossing occurs during transport. The process $\nu(t)$ is in general non-differentiable, because it displays variations on arbitrary small timescales (like e.g. the standard Brownian motion). We call $\nu(t)$ a "slow process" in the following sense: over a time interval Δt of order ϵ , the variations of the stochastic process scale as $\Delta \nu \propto \sqrt{\epsilon \Delta t}$, and are thus very small compared to the variations of canonical variables. Variations $\Delta \nu$ of order one only occur on a timescale Δt of order one. With this signification, ϵ creates a timescale separation between the Hamiltonian dynamics and the stochastic dynamics of ν . We call ϵ the "fast timescale", as opposed to the natural timescale of order one to describe the system, that we call the "slow timescale". The time evolution of $\nu(t)$ is given by

$$d\nu = a(\nu)dt + b(\nu)dW. \quad (6)$$

In the stochastic differential equation (6), the stochastic product $b(\nu)dW$ is defined with the Itô convention of stochastic calculus (see [32] chapter 4). We again strongly emphasize that the variable $\nu(t)$ is not a slow variable in the usual sense, because its motion contains infinitely fast variations. It can only be considered as "slow" in the sense that its time-integrated variations $\Delta \nu = \int_0^{\Delta t} \dot{\nu}(s)ds$ are much smaller than the variations of $\{p, q\}$ over the same time interval.

As the Hamiltonian $H(p, q, \nu)$ is integrable for fixed ν , we can find a set of action-angle canonical variables (P, Q) . With this change of variables, the new Hamiltonian $\tilde{H}(P, \nu)$ does not depend on Q . If the value of ν is fixed, the action variable $P(p, q, \nu)$ is a constant of motion under the dynamics of the Hamiltonian \tilde{H} . In the model defined by equations (5-6), the parameter ν follows a stochastic differential equation. This implies that the action variable P also follows a stochastic differential equation, and evolves on the same timescale as $\nu(t)$. Using the principles of Itô stochastic calculus, the stochastic differential equations on P and Q are

$$\begin{cases} dP &= -\frac{1}{\epsilon} \frac{\partial P}{\partial p} \frac{\partial H}{\partial q} dt + \frac{1}{\epsilon} \frac{\partial P}{\partial q} \frac{\partial H}{\partial p} dt + \frac{\partial P}{\partial \nu} [a(\nu)dt + b(\nu)dW] + \frac{1}{2} \frac{\partial^2 P}{\partial \nu^2} b^2(\nu)dt, \\ dQ &= -\frac{1}{\epsilon} \frac{\partial Q}{\partial p} \frac{\partial H}{\partial q} dt + \frac{1}{\epsilon} \frac{\partial Q}{\partial q} \frac{\partial H}{\partial p} dt + \frac{\partial Q}{\partial \nu} [a(\nu)dt + b(\nu)dW] + \frac{1}{2} \frac{\partial^2 Q}{\partial \nu^2} b^2(\nu)dt. \end{cases} \quad (7)$$

Because the set (P, Q) is a set of action-angle variables, the term $-\frac{\partial P}{\partial p} \frac{\partial H}{\partial q} dt + \frac{\partial P}{\partial q} \frac{\partial H}{\partial p} dt$ vanishes. This comes as a consequence of the fact that P is constant if ν is constant. The term $-\frac{\partial Q}{\partial p} \frac{\partial H}{\partial q} dt + \frac{\partial Q}{\partial q} \frac{\partial H}{\partial p} dt$ defines the dynamics of the angle variable Q when ν is fixed, and thus

$$-\frac{\partial Q}{\partial p} \frac{\partial H}{\partial q} dt + \frac{\partial Q}{\partial q} \frac{\partial H}{\partial p} dt = \omega(P, \nu)dt,$$

where we have defined the pulsation $\omega(P, \nu) := \frac{\partial \tilde{H}}{\partial P}(P, \nu)$. Equations (6-7) become

$$\begin{cases} dP &= \left[\frac{\partial P}{\partial \nu} a(\nu) + \frac{1}{2} \frac{\partial^2 P}{\partial \nu^2} b^2(\nu) \right] dt + \frac{\partial P}{\partial \nu} b(\nu) dW, \\ dQ &= \frac{1}{\epsilon} \omega(P, \nu) dt + \left[\frac{\partial Q}{\partial \nu} a(\nu) + \frac{1}{2} \frac{\partial^2 Q}{\partial \nu^2} \epsilon b^2(\nu) \right] dt + \frac{\partial Q}{\partial \nu} b(\nu) dW, \end{cases} \quad (8)$$

and

$$d\nu = a(\nu) dt + b(\nu) dW.$$

The set (P, Q, ν) evolves according to a slow-fast dynamics: the angle variable Q evolves on a timescale of order ϵ , whereas the variables P and ν evolving on a timescale of order one. Our aim is to average the system (8) over the dynamics of Q to obtain a closed system of equations describing the dynamics of (P, ν) .

Before doing the averaging procedure, we first recall a very classical result of Hamiltonian systems with slow time dependence (see e.g [23] or [2] section 2.3). There exists a smooth function $H_1(P, Q, \nu)$ such that the differential of (P, Q) with respect to ν can be expressed as

$$\begin{cases} \frac{\partial P}{\partial \nu} &= -\frac{\partial H_1}{\partial Q}, \\ \frac{\partial Q}{\partial \nu} &= \frac{\partial H_1}{\partial P}. \end{cases} \quad (9)$$

We propose a simple proof of this result in Appendix B using differential two-forms. With the important result (9), we can compute the second order differential of P using the differentials of H_1 . We define the canonical Poisson brackets of any functions $f(p, q)$ and $g(p, q)$ by

$$\{f, g\}_{p,q} := \frac{\partial f}{\partial p} \frac{\partial g}{\partial q} - \frac{\partial f}{\partial q} \frac{\partial g}{\partial p}.$$

We have

$$\begin{aligned} \frac{\partial^2 P}{\partial \nu^2} &= \frac{\partial}{\partial \nu} \left(-\frac{\partial H_1}{\partial Q} \right) \\ &= -\frac{\partial^2 H_1}{\partial P \partial Q} \frac{\partial P}{\partial \nu} - \frac{\partial^2 H_1}{\partial Q^2} \frac{\partial Q}{\partial \nu} - \frac{\partial^2 H_1}{\partial \nu \partial Q}, \end{aligned}$$

and using once more (9) we obtain

$$\frac{\partial^2 P}{\partial \nu^2} = -\left\{ H_1, \frac{\partial H_1}{\partial Q} \right\}_{P,Q} - \frac{\partial^2 H_1}{\partial \nu \partial Q},$$

with $\left\{ H_1, \frac{\partial H_1}{\partial Q} \right\}_{P,Q}$ the canonical Poisson bracket with the set of variables (P, Q) . A similar computation leads to

$$\frac{\partial^2 Q}{\partial \nu^2} = \left\{ H_1, \frac{\partial H_1}{\partial P} \right\}_{P,Q} + \frac{\partial^2 H_1}{\partial \nu \partial P}.$$

We write the slow-fast system of equations (8) as

$$\begin{cases} dQ &= \frac{1}{\epsilon} \omega(P, \nu) dt + \text{terms of order 0 in } \frac{1}{\epsilon}, \\ dP &= \left[-\frac{\partial H_1}{\partial Q} a(\nu) - \frac{1}{2} \left(\left\{ H_1, \frac{\partial H_1}{\partial Q} \right\}_{P,Q} + \frac{\partial^2 H_1}{\partial \nu \partial Q} \right) b^2(\nu) \right] dt - \frac{\partial H_1}{\partial Q} b(\nu) dW, \\ d\nu &= a(\nu) dt + b(\nu) dW. \end{cases} \quad (10)$$

We are now in position of doing the averaging procedure for the system (10). The averaging should be done with particular rules, as we are dealing with a stochastic system. There are two standard methods of averaging for such a stochastic system. The first one consists in writing the Fokker-Planck equation corresponding to (10), and then find the limit of this equation when $\epsilon \rightarrow 0$ using an expansion in powers of ϵ . This method is well described in the literature and can for example be found in [33, 34]. In the following, we use another fully equivalent method (in the spirit of the techniques used by [35, 12, 36]), in which we directly average the different terms in (10).

We want to average the dynamics of P over the fast dynamics of the angle Q . To leading order in $\frac{1}{\epsilon}$, the dynamics of Q is simply

$$\dot{Q} = \frac{1}{\epsilon} \omega(P, \nu).$$

Therefore, the invariant measure of this dynamics, for any fixed values of P and ν , is just the constant measure over the range $[0, 2\pi]$. To find the limit stochastic process for P when ϵ goes to zero, we have to average equation (10) using the invariant measure of Q . Some terms are very easy to compute. Let $\langle \cdot \rangle_Q := \frac{1}{2\pi} \int_0^{2\pi} \cdot dQ$ be the averaging operator over the fast dynamics of Q , we have

$$\left\langle \frac{\partial H_1}{\partial Q} \right\rangle_Q = 0 \quad \text{and} \quad \left\langle \frac{\partial^2 H_1}{\partial \nu \partial Q} \right\rangle_Q = 0.$$

In the deterministic part on the equation for P , the only nonzero dependance comes from the average of the Poisson bracket $\left\langle \left\{ H_1, \frac{\partial H_1}{\partial Q} \right\} \right\rangle_Q$.

The average of the stochastic term $\frac{\partial H_1}{\partial Q} b(\nu) dW$ is more subtle, because it involves the stochastic process $W(t)$ that has variations on very small timescales. We detail the full procedure in Appendix A. The main idea is that the sum of independent Gaussian random variables is still a Gaussian random variable. As a consequence of this property, the average of the Gaussian white noise $\frac{\partial H_1}{\partial Q} b(\nu) dW$ is still a Gaussian white noise, because the average is composed of a sum of infinitely small Gaussian increments. For the standard Brownian motion for example, this property implies that $W(t)$ is self-similar, namely that for all $\tau > 0$, $W(t/\tau) = (1/\sqrt{\tau})W(t)$. Because of the property of self-similarity, a diffusion process is never slow in the strong sense. It can be considered as "slow" in the sense that its probability density evolves on a slow timescale. More details are given in Appendix A.

To average over Q , we introduce first the matrix

$$\sigma := \begin{pmatrix} b(\nu) \\ b(\nu) \frac{\partial H_1}{\partial Q} \end{pmatrix}.$$

The noise term acting on the set of slow variables (ν, P) can be written as σdW , where W is a Wiener process. We then use the standard result that the noise term

$$\sigma \left(Q \left(\frac{t}{\epsilon} \right) \right) dW$$

is equivalent (for the probability distribution) when $\epsilon \rightarrow 0$ to a Gaussian white noise process, the variance of which is given by the averaged correlation matrix $\langle \sigma \sigma^T \rangle_Q$ (see e.g [12] chapter 8, and Appendix A). The correlation matrix of the noise is

$$\sigma \sigma^T = \begin{pmatrix} b^2(\nu) & b^2(\nu) \frac{\partial H_1}{\partial Q} \\ b^2(\nu) \frac{\partial H_1}{\partial Q} & b^2(\nu) \left(\frac{\partial H_1}{\partial Q} \right)^2 \end{pmatrix},$$

and averaging over Q gives

$$\langle \sigma \sigma^T \rangle_Q = \begin{pmatrix} b^2(\nu) & 0 \\ 0 & b^2(\nu) \left\langle \left(\frac{\partial H_1}{\partial Q} \right)^2 \right\rangle_Q \end{pmatrix}. \quad (11)$$

The important consequence of (11) is that the average over the fast dynamics eliminates the correlations between the noise terms in the equations of P and ν .

We can now present our main theoretical result. The dynamics of the slow process (P, ν) follows when ϵ goes to zero the averaged equations

$$\begin{cases} dP &= -\frac{1}{2} b^2(\nu) \left\langle \left\{ H_1, \frac{\partial H_1}{\partial Q} \right\} \right\rangle_Q dt + b(\nu) \sqrt{\left\langle \left(\frac{\partial H_1}{\partial Q} \right)^2 \right\rangle_Q} dW_1, \\ d\nu &= a(\nu) dt + b(\nu) dW_2. \end{cases} \quad (12)$$

There are some interesting comments to do on equations (12).

1. First, we note that the Wiener processes W_1 and W_2 involved in the two equations for P and ν are independent. This beautiful property is a consequence of the relation $\frac{\partial P}{\partial \nu} = -\frac{\partial H_1}{\partial Q}$. It seems counterintuitive that two independent Wiener processes can appear as the limit of a single Wiener process. We can heuristically explain this result as follows. A large "kick" created by the Wiener process is in fact the cumulative result of a large number of small "kicks" (see A for a more detailed description). But because of the presence of the amplitude $\frac{\partial H_1}{\partial Q}$ in the equation for P , each "kick" is weighted by a particular value of $\frac{\partial H_1}{\partial Q}$, and the sum is composed

of terms that cancel each other. A large kick in the equation for ν is not felt by the action P because the cumulative effect is destroyed by the weight function $\frac{\partial H_1}{\partial Q}$. Therefore, noise-stimulated events for ν and P are related to completely different realizations of the Wiener process. It would not be the case if we had chosen to study the dynamics of another slow variable of the system, for example the Hamiltonian H .

2. Also, we observe that the diffusion of the action P only comes from the stochastic part of the equation for ν , the coefficient $b(\nu)$. For a smooth function $\nu(t)$, the action cannot diffuse. This is in accordance with the theory of adiabatic invariants, that states that for a smooth time dependance of $\nu(\epsilon t)$, there exists an adiabatic invariant conserved to any order in ϵ (This result was found by [22] for the harmonic oscillator, and [23] in the general case). In the case where such an invariant exists, the action cannot diffuse.

An other interesting remark is that the stochastic equation (12) for P can be written in a more compact way. From the relation

$$\frac{\partial}{\partial Q} \left(\frac{\partial H_1}{\partial P} \frac{\partial H_1}{\partial Q} \right) = \frac{\partial H_1}{\partial P} \frac{\partial^2 H_1}{\partial Q^2} + \frac{\partial^2 H_1}{\partial Q \partial P} \frac{\partial H_1}{\partial Q}$$

averaged over Q , we get

$$\left\langle \frac{\partial H_1}{\partial P} \frac{\partial^2 H_1}{\partial Q^2} \right\rangle_Q = - \left\langle \frac{\partial^2 H_1}{\partial Q \partial P} \frac{\partial H_1}{\partial Q} \right\rangle_Q. \quad (13)$$

Using (13), equation (12) for P can be equivalently written

$$dP = b^2(\nu) \frac{\partial}{\partial P} \left\langle \left(\frac{\partial H_1}{\partial Q} \right)^2 \right\rangle_Q dt + b(\nu) \sqrt{\left\langle \left(\frac{\partial H_1}{\partial Q} \right)^2 \right\rangle_Q} dW_1.$$

Interestingly, the last equation shows that the drift and the noise amplitude are related to the same function, and that one can be obtained from the other.

In the following section 2.2, we present a simple applications of the theoretical result (12). We study the well-known harmonic oscillator with random frequency, which allows for explicit computations.

2.2 Application to the harmonic oscillator

The Hamiltonian of the harmonic oscillator is

$$H(p, q, \nu) = \frac{1}{2}p^2 + \frac{1}{2}\nu^2 q^2. \quad (14)$$

and the set of Hamilton's equations (2) that describes the dynamics of the canonical variables (p, q) on the slow timescale is

$$\begin{cases} \dot{p} &= -\frac{1}{\epsilon} \frac{\partial H}{\partial q}(p, q, \nu(t)) \\ \dot{q} &= \frac{1}{\epsilon} \frac{\partial H}{\partial p}(p, q, \nu(t)) \end{cases} \quad (15)$$

We consider that the frequency of the oscillator ν is a parameter in the Hamiltonian (14), which time evolution is given by the Itô stochastic differential equation

$$d\nu = a(\nu)dt + b(\nu)dW. \quad (16)$$

The small parameter $\epsilon \ll 1$ sets the timescale separation between the Hamiltonian dynamics, and the dynamics of the random frequency. Equations (15-16) define our model.

We introduce the classical action-angle variables (P, Q) defined by the relations

$$\begin{aligned} p &= \sqrt{2\nu P} \cos Q, \\ q &= \sqrt{\frac{2P}{\nu}} \sin Q, \end{aligned} \quad (17)$$

and the new Hamiltonian $\tilde{H}(P, \omega)$ simply becomes

$$\tilde{H}(P, \nu) = \nu P.$$

To use the result (12), we have to find the expression of H_1 as a function of P, Q and ν . From the expression $P = \frac{p^2}{2\nu} + \frac{\nu q^2}{2}$ we compute

$$\begin{aligned}\frac{\partial P}{\partial \nu} &= -\frac{1}{2\nu^2}p^2 + \frac{1}{2}q^2 \\ &= -\frac{1}{\nu}P \cos^2 Q + \frac{1}{\nu}P \sin^2 Q \\ &= -\frac{\partial}{\partial Q} \left[\frac{1}{2\nu}P \sin(2Q) \right].\end{aligned}$$

A straightforward calculation also shows that

$$\begin{aligned}\frac{\partial Q}{\partial \nu} &= \frac{1}{2\nu} \sin(2Q) \\ &= \frac{\partial}{\partial P} \left[\frac{1}{2\nu}P \sin(2Q) \right].\end{aligned}$$

This gives the function $H_1(P, Q, \nu)$ ([2] section 2.3)

$$H_1 = \frac{1}{2\nu}P \sin(2Q).$$

In the case of the harmonic oscillator, equations (12) are explicitly

$$\begin{cases} dP &= b^2(\nu) \frac{P}{2\nu^2} dt + b(\nu) \frac{P}{\sqrt{2\nu}} dW_1, \\ d\nu &= a(\nu) dt + b(\nu) dW_2. \end{cases} \quad (18)$$

In order to illustrate the result (18), we perform a numerical simulation. We have to choose a stochastic process. We choose a process such that the frequency ν is always strictly positive, otherwise action variables are ill-defined. We thus set $b(\nu) = \sqrt{2\sigma^2}$, where σ is a constant parameter, and $a(\nu) = -\nabla V(\nu)$, where the potential $V(\nu) = \frac{1}{\nu} + \frac{1}{\nu_{max} - \nu}$ is chosen such that the frequency ν is trapped in the range $]0, \nu_{max}[$.

We integrate Hamilton's equations of motion

$$\begin{cases} \dot{q} &= \frac{1}{\epsilon} p, \\ \dot{p} &= -\frac{\nu^2}{\epsilon} q, \end{cases}$$

using a symplectic integrator of order 2. And we integrate simultaneously the stochastic equation for ν

$$d\nu = \left[\frac{1}{\nu^2} - \frac{1}{(\nu_{max} - \nu)^2} \right] dt + \sqrt{2\sigma^2} dW,$$

using a stochastic Euler algorithm (described e.g. in [32] chapter 15). The integration is done over 10,000 realizations of the stochastic frequency, and the same initial conditions $(p_0, q_0) = (1, 0)$, $\nu_0 = \frac{\nu_{max}}{2}$ for each trajectory. The parameters are $\nu_{max} = 2.0$, $\sigma = 0.3$ and $\epsilon = 0.01$. The histogram of the action $P = \frac{p^2}{2\nu} + \frac{\nu q^2}{2}$ is represented at different times on figure (2) by the histograms.

Secondly, we perform 10,000 integrations of the averaged equations

$$\begin{cases} dP &= \sigma^2 \frac{P}{\nu^2} dt + \sigma \frac{P}{\nu} dW_1, \\ d\nu &= \left[\frac{1}{\nu^2} - \frac{1}{(\nu_{max} - \nu)^2} \right] dt + \sqrt{2\sigma^2} dW_2, \end{cases}$$

with the same parameters and initial conditions. The histogram of the action is represented by the curve on figure (2). Both agree up to sampling errors, as expected. The main interest of using the averaged equations to compute a PDF is of course the drastic reduction of the time of integration. Moreover, one can then recover the PDF of the initial variables (p, q) using the change of variable and the fact that the PDF of Q is uniform over $[0, 2\pi]$.

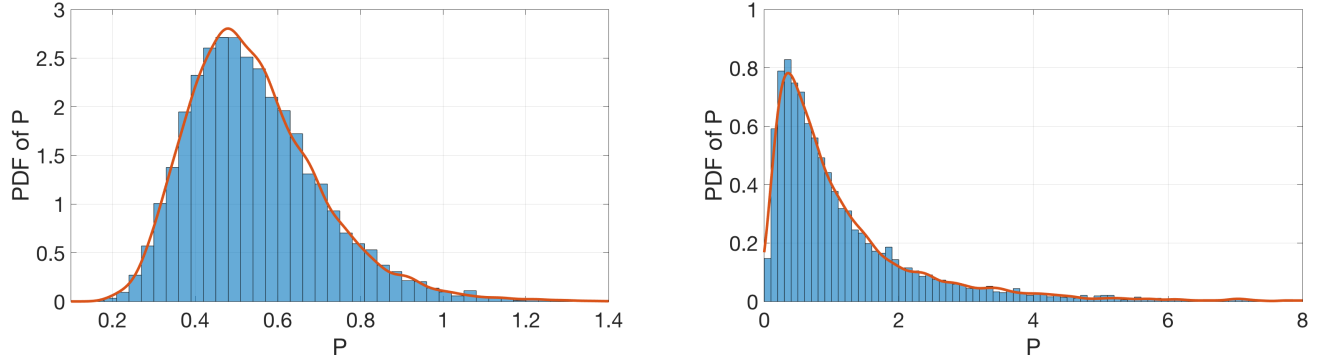


Figure 2: PDF of the canonical action P obtained either with Hamilton's equations (histogram) or with the averaged equations (curve), at $t = 50$, and $t = 500$.

3 The chaotic case

3.1 Formulation of the model

We now turn to a more difficult situation. We study the dynamics (2) where the Hamiltonian $H(x, \nu)$ has one and a half degrees of freedom. More precisely, the set of canonical variables is $\{(p, q), (\Lambda, \lambda)\}$ but Λ does not play any role in the dynamics. We assume that the explicit time dependence in H creates many resonances overlap, and thus the Hamiltonian dynamics for fixed ν has both regular and chaotic trajectories. The phase space is divided into regions with different mixing properties. In the regions in (p, q) -space where at least two resonances overlap, the dynamics is strongly chaotic. In regions of phase space that are far away from the main resonances, the dynamics is almost regular. KAM-tori may subsist or not, depending on the amplitude and localization of the resonant frequencies. The parameter ν is assumed to be stochastic, and evolving on a time scale of order one, whereas the canonical variables evolve on the small timescale $\epsilon \ll 1$. We want to characterize transport in phase space on the slow timescale.

By contrast with the simplest integrable case of section 2, there is now no global action variable. The transport cannot be described by a diffusive equation of some kind of action variable. What we will explain in the present section is that the transport is very different in the present case where the dynamics of H is chaotic. In the chaotic case, there are two competitive transport mechanisms, that can be qualitatively described as follows:

1. The chaotic regions are moving in phase space. If the system is in one of those chaotic regions, it is carried together with the region upwards or downwards. At any time, it can leave the region and enter in the regular part of phase space. But depending on when the system leaves the region, it may be carried up or down far away from its initial position. We refer to this mechanism as “transport by migration with chaotic regions”.
2. The regular regions far away from the resonances are very similar to the integrable Hamiltonian dynamics of section 2. The slow stochastic variations of ν distort the orbits, and enhances the chaotic diffusion of these regions. As a result, no KAM tori can subsist and the system diffuses through phase space on a time scale of order one. We refer to this mechanism as “noise driven transport in regular regions”.

Depending on the parameters of the Hamiltonian, one of the two mechanisms described above may overcome the other. This section provides a concrete example of a Hamiltonian where the two mechanisms of transport are present. We also determine in which parameter regime the transport by migration with chaotic regions is dominant.

We propose to study the Hamiltonian dynamics (2), where the Hamiltonian depends on a set of four frequencies

$$H(p, q, \Lambda, \lambda, \nu) = \frac{p^2}{2} + \sum_{k=1}^4 \cos(q - \lambda_k - \varphi_k) + \sum_{k=1}^4 \nu_k \Lambda_k, \quad (19)$$

Where $\{\Lambda, \lambda\}$ are now conjugated canonical variables of dimension four. The dynamics (2) is explicitly

$$\begin{cases} \dot{q} &= \frac{1}{\epsilon} p \\ \dot{p} &= \frac{1}{\epsilon} \sum_{k=1}^4 \sin(q - \lambda_k - \varphi_k) \\ \dot{\lambda} &= \frac{1}{\epsilon} \nu \end{cases} \quad (20)$$

frequencies ν_k^* (s^{-1})	initial angles φ_k	timescale separation ϵ
10.0	0.0	10 ⁻²
9.9	π	
0.1	π	
0.0	0.0	

Table 1: Fixed parameters of the model (19-21)

The canonical action Λ does not play any role in the dynamics. The set of four frequencies $\nu := (\nu_1, \nu_2, \nu_3, \nu_4)$ plays the role of the external parameters. The frequencies are divided in two groups of two frequencies which create resonance overlap, and create two main chaotic regions around $p = 0$ and $p = 10$ respectively. The parameters $\{\varphi_k\}_{k=1..4}$ are some initial phases, and ϵ is a small parameter to model the timescale separation between the fast dynamics of the canonical variables and the stochastic dynamics of the frequencies. To complete our Hamiltonian model (19), we need to specify the stochastic process for the set of frequencies ν . We choose for the variations of ν an Ornstein-Uhlenbeck process defined by

$$d\nu = -(\nu - \nu^*)dt + \sqrt{2\sigma^2}dW. \quad (21)$$

In Equation (21), $W(t)$ is a 4-dimensional Wiener process. In order to keep the size of the stochastic regions constant, we choose to prescribe the same noise for two frequencies of the same set, that is, $W_1 = W_2$ and $W_3 = W_4$. The correlation function of the noise is $\langle dW_1(t)dW_3(t') \rangle = 0$ and $\langle dW_1(t)dW_1(t') \rangle = \langle dW_3(t)dW_3(t') \rangle = \delta(t-t')dt$. The parameter σ quantifies the noise amplitude and is the same for all frequencies. The term $-(\nu - \nu^*)$ keeps the frequencies close to their averaged values defined by the set ν^* . The choice to keep pairs of frequencies with the same noise has no physical justification, it is only a simplifying assumption to keep constant the widths of the chaotic regions. In the general case, we expect both the width and the position of the chaotic regions to vary with time. If the frequencies of a pair do not have the same noise, a mechanism of transport by slow extension of the chaotic regions occurs. However, this third mechanism is very similar to the mechanism of transport through slow migration of chaotic regions, and can be accounted for using the same techniques as the ones presented in this section. An extension of the theory to the general case is left apart for further work.

The Hamiltonian (19) together with the stochastic equation (21) completely defines our model. In the simulations of the dynamics (20), the parameters φ_k , the timescale separation ϵ and the mean frequencies ν_k^* were fixed to the values given in table (1), whereas the amplitude σ is a control parameter that we changed in the different simulations.

In figure (3), we have represented two pictures to help the reader understand the chaotic structure of phase space. On the left, we have represented the cat's eyes of the main resonances in red. All the regions of phase space covered by the eyes are strongly chaotic. The two first order resonances appear with amplitude 1 in the Hamiltonian (19), and thus create cat's eyes with extension 4. The second order resonances create a chaotic region around $p = 5$, and its extension can be found using Lie transformations of the Hamiltonian (19). We found that the second order resonances come with typical amplitude $\frac{2}{\nu_1^2}$ and have thus an extension $4\sqrt{\frac{2}{\nu_1^2}} \approx 0.56$. Those three chaotic regions are separated by two regular bands, in which transport is only possible either through the weak chaos created by higher order resonances, that are of much smaller amplitudes, or through noise driven transport in regular regions. On the right of figure (3), we have represented the bands associated with the chaotic regions of first and second orders. For convenience, we have labelled the regions. Regions 1 and 2 are the chaotic regions of first order resonances, and region 3 is the chaotic region of second order resonances. The regions of weak chaos, which we also call the "regular" regions, are labelled as regions 4 and 5. Within the bands 1, 2 and 3, chaos is strongly developed, and the system is thus rapidly carried throughout the band on the timescale ϵ . The bands are separated by regions 4 and 5 of much weaker chaos: for fixed values of the frequencies ν , the system can hardly cross those regular regions, and therefore the migration between one band to the other is very slow.

The important point to emphasize is that figure (3) is not static: the set of four frequencies ν is slowly varying around its mean values ν^* , with stochastic variations defined by equation (21). This slow variation of the frequencies imply that the transport in phase space does not only happen through the well known "chaotic diffusion" observed in chaotic maps (e.g the standard map, see [2] chapter 5). It comes from two other mechanisms that we have previously referred to as "transport by migration with chaotic regions" and "noise driven transport in regular regions". We look in section 3.4 at the problem of first passage time at $p = 0$ starting at $p = 10$. We will see that the first mechanism, that is, transport by migration with the chaotic regions, is dominant for large noise amplitude.

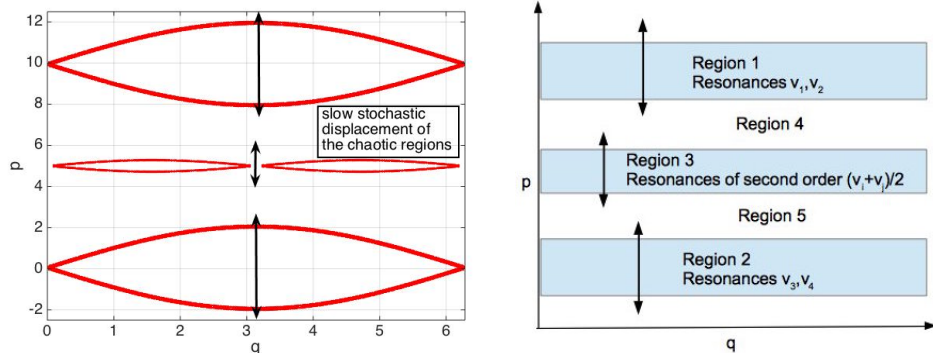


Figure 3: Schematic representation of the chaotic structure of phase space for the Hamiltonian (19). The left panel represents The eyes of the resonances of first and second order in the system. Resonance overlap creates strongly chaotic regions in phase space. The chaotic regions are represented by the bands on the right panel. The arrows indicate that the chaotic regions are slowly moving with time.

Let us assume for example that we are in a range of parameters for which the transport is mainly due to migration with the chaotic regions. The system starts at $p = 10$. It can reach the value $p = 0$ through successive jumps from one region to the other, until it eventually reaches the chaotic region around the frequency $\nu_4^* = 0$. To illustrate the transport mechanism, we have represented in figure (4) the different steps of the transport. We have labelled the chaotic and regular regions the same way as in figure (3). First, one downward fluctuation of the couple of frequencies (ν_1, ν_2) brings together the chaotic region 1 and the system around $p = 7$. Then, region 1 moves upward again, but the system leaves the chaotic region and is thus trapped in region 4. A simultaneous displacement upwards of the frequencies ν_3 and ν_4 brings the region 3 of second order resonances upwards, and it captures the system. The system has thus passed from region 1 to region 3 thanks to stochastic migration with the chaotic regions. It then passes from region 3 to region 2 by a similar trajectory mechanism: it is transported downwards and left in region 5 and an eventual upward displacement of region 2 captures it and brings it to $p = 0$. Figure (5) displays an example of a trajectory starting at $p = 10$ and reaching $p = 0$. The example of figure (5) shows that transport is not straightforward to $p = 0$. The system can be captured and released many times by a chaotic region before being captured by another chaotic region. In the example of figure (5), the system spends most of the time in the vicinity of region 1, and the transition to regions 3 and 2 only occurs at the very end of the trajectory.

The mechanism of transport we just described, composed of successive jumps between regions of different types, is typical to go from $p = 10$ to $p = 0$ when chaotic diffusion in the regular regions is negligible. As the reader would surely have noticed, it is not important where the system is exactly located when it is inside a chaotic region of type 1, 2 or 3. The mixing in those strongly chaotic regions is so fast compared to the timescale of frequency variations, that the system has time to explore the whole region before any significant displacement of the region. To say it another way, the underlying Hamiltonian dynamics is not important to determine the transport characteristics. In fact, there are only two properties of the dynamics that matter. The first one is the conservation of area which is characteristic of Hamiltonian dynamics (the Hamiltonian flow is a symplectic transformation). The second one is that the phase space is partitioned into several strongly mixing regions (where chaos is strongly developed), separated by regular regions. Those two properties prompted us to perform a kind of “averaging” of the Hamiltonian dynamics and build an even simpler, fully stochastic model, that we call the *local diffusion model*.

3.2 Averaging of the dynamics: the local diffusion model

The local diffusion model is a purely stochastic model built from the Hamiltonian model (19) with stochastic frequencies (21). The idea is to average the dynamics over an intermediate timescale which is much longer than the timescale of the Hamiltonian dynamics, but much smaller than the timescale of stochastic variations of the frequencies. We use the hypothesis that the regions of strong chaos are also mixing. As the timescale of the Hamiltonian dynamics is typically of order $\frac{1}{\nu_1^*}$, the averaging procedure is done over a time τ_{av} satisfying

$$\frac{\epsilon}{\nu_1^*} \ll \tau_{av} \ll \frac{1}{\nu_1^*}. \quad (22)$$

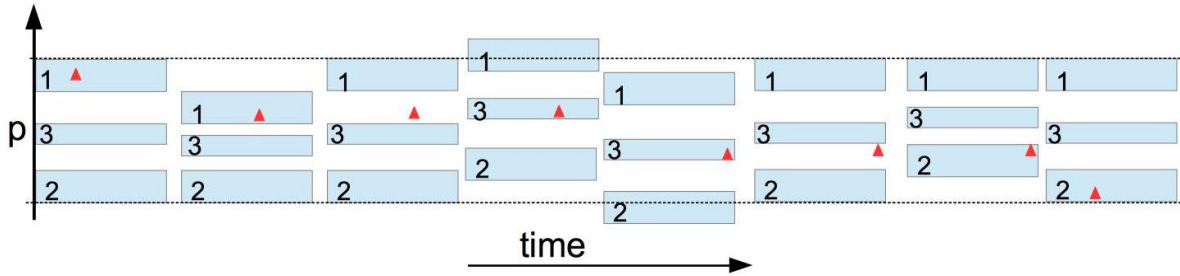


Figure 4: Schematic representation of a trajectory in the Hamiltonian stochastic model (19). The system is represented by the red triangle. The picture displays the chaotic regions 1, 2 and 3 at 8 different times. The system is initially located in region 1 and is carried to region 2 through the mechanism of transport by migration of the chaotic regions.

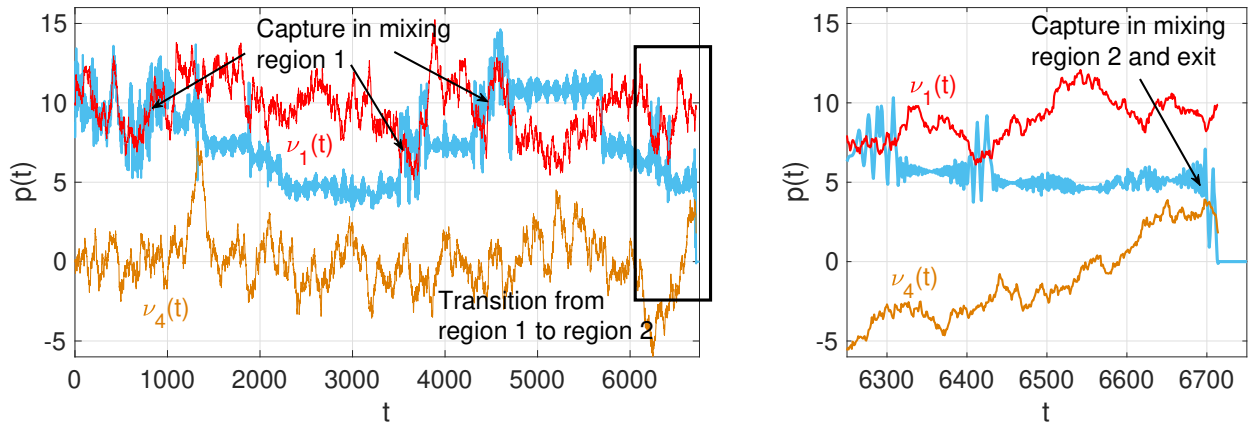


Figure 5: Example of a trajectory in the stochastic Hamiltonian model (19) transported from $p = 10$ to $p = 0$ by the stochastic migration of the chaotic regions. The blue curve is the action $p(t)$. The red and orange curves represent the frequencies $\nu_1(t)$ and $\nu_4(t)$. When the system is located in the chaotic region 1, the action value has fast and large fluctuations around $\nu_1(t)$. When the system leaves region 1 and enters in the weakly chaotic region 4, the action fluctuations are much smaller. The left panel is an enlargement of the end of the trajectory, when the system is captured by the chaotic region 2 and exits through the boundary at $p = 0$.

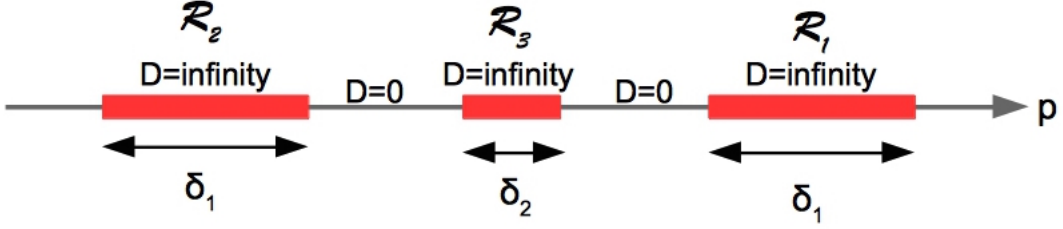


Figure 6: Schematic representation of the local diffusion model. The regions 1, 2 and 3 with infinite diffusion coefficients are displayed by the red rectangles.

Over the timescale τ_{av} , the Hamiltonian dynamics in the chaotic regions is assumed to be mixing. Strong chaos separates the neighboring trajectories exponentially fast, on a timescale of order $\frac{c}{\nu^*}$, and the system has thus completely “forgotten” its initial condition over the timescale τ_{av} . This means that if the system has an initial condition inside the chaotic region 1 of figure (4) (for example), it can be anywhere inside the region 1 after a time τ_{av} . On the other hand, we assume that chaos is weak enough in the regular regions 4 and 5 of figure (4) to keep the system to an average value very close to p within the time τ_{av} .

The local diffusion model of second order is represented in figure (6). It consists of three patches of infinite diffusion coefficient D in p -space. Two of them have an extension δ_1 , and correspond in figure (3) to the chaotic regions 1 and 2 of main resonances. The third one has a smaller extension δ_2 and corresponds to region 3 of second order resonances in figure (3). We assume that chaotic transport is negligible away from the resonances of first and second orders, that’s why we set the diffusion coefficient to zero out of the diffusion patches. The diffusion patches are then moved according to the stochastic dynamics (21).

The solution cannot be represented any more by a trajectory, but only through the probability distribution $\rho_\nu(p, t)$ to find the system at impulsion p at time t , given a realization of the stochastic process $\nu(t)$. Let δ_i be the extension of the i -th diffusion region that we call \mathcal{R}_i . The diffusion region \mathcal{R}_i then covers the interval $[\nu_i - \delta_i/2, \nu_i + \delta_i/2]$. If the impulsion p is out of all the diffusion regions, the function $\rho_\nu(p, t)$ remains the same at step $t + dt$. If p is inside the diffusion region \mathcal{R}_i , the probability distribution at step $t + dt$ is the average of the probability distribution over the whole region. The dynamics of the distribution $\rho_\nu(p, t)$ can be implemented following the equations

$$\rho_\nu(p, t + dt) = \begin{cases} \frac{1}{\delta_i} \int_{\nu_i(t) - \delta_i/2}^{\nu_i(t) + \delta_i/2} \rho_\nu(p', t) dp' & \text{if } p \text{ is in region } \mathcal{R}_i \\ \rho_\nu(p, t) & \text{otherwise} \end{cases} \quad (23)$$

$$\nu(t + dt) = \nu(t) - (\nu - \nu^*)dt + \sqrt{2\sigma^2}dW(t) \quad (24)$$

The second equation (24) is just another way to write Equation (21). We have $dW_1 = dW_2$, $dW_3 = dW_4$, and $\langle dW_1(t)dW_1(t') \rangle = \delta(t - t')dt$ and $\langle dW_1(t)dW_3(t') \rangle = 0$. The consequence of equation (23) is that at each step, the probability distribution is constant over each region \mathcal{R}_i . But as the reader can see on equation (23), the region \mathcal{R}_i is moving because of the variations of the frequencies $\{\nu_i\}_{i=1..4}$. Therefore, at the next step, the average is performed over a region which has slightly moved during the time step dt .

3.3 The Markov process that corresponds to the local diffusion model

In this section, we give a rigorous mathematical definition of the process described by equations (23-24). We explain that there is no proper Markov process for the variable (p, ν) corresponding exactly to equations (23-24) but that an equivalent Markov process exists on an extended space. For simplicity, we define the Markov process for a single diffusion region \mathcal{R} , but the following discussion can be straightforwardly generalized to many diffusion regions.

Let us consider the stochastic process (p_t, ν_t) defined by the following rules. First, $d\nu_t = -(\nu_t - \nu^*)dt + \sqrt{2\sigma^2}dW(t)$, and then p_t is a jump process such that if $p_t \in \mathcal{R}$ then p_t jumps to any other point of \mathcal{R} at a rate

$1/(\epsilon\delta)$ (where δ is the width of the diffusion region), and that if p_t does not belong to \mathcal{R} then it stays constant. This defines a Markov process. One can think of ϵ as being the same as in section 3.1, or being another unrelated parameter. One can write the infinitesimal generator of this process. If ϕ is a test function on the space (p, ν) , then the infinitesimal generator is

$$G_{(p,\nu)}[\phi] = \frac{1}{\epsilon} \left[\frac{1}{\delta} \int_{\nu-\delta/2}^{\nu+\delta/2} \phi(p_1, \nu) dp_1 - \phi(p, \nu) \right] I_{\mathcal{R}}(p) + L_{\nu}[\phi], \quad (25)$$

where $I_{\mathcal{R}}(p)$ is the step function equal to 1 if $p \in \mathcal{R}$ and zero otherwise, and L_{ν} is the infinitesimal generator of the diffusion (24).

The process described by (23-24) corresponds to the infinite rate limit ($\epsilon \rightarrow 0$ or $1/\epsilon \rightarrow \infty$) of the process with infinitesimal generator (25). We could equivalently say that (23-24) is the infinite rate limit of the finite rate jump process (25). As is clearly seen from (25), the infinitesimal generator (25) does not have a simple limit when $\epsilon \rightarrow 0$. In this limit, when p_t is inside \mathcal{R} , it oscillates faster and faster, uniformly over the set \mathcal{R} . In order to define properly the limit for such a fast oscillating variable, we would need the formalism of Young measures and weak convergence.

For finite ϵ , we first define a Markov process over the space of measures as follows: we first regularize the process ν_t by introducing a correlation time τ_c , and ν_t is the diffusion process

$$\dot{\nu}_t = -(\nu_t - \nu^*) + \sqrt{2\sigma^2}\eta(t), \quad (26)$$

where η is a continuous random process such that $\langle \eta(t), \eta(t') \rangle = \frac{1}{\tau_c} e^{-t/t'}$. With the above definition, the velocity $\dot{\nu}_t$ is a well-defined variable. The mixing region is still defined as $\mathcal{R}_t := [\nu_t - \delta/2, \nu_t + \delta/2]$. Then we introduce the process μ_t in the space of measures and the jump process $p_t^0 \in \mathbb{R}$ with the following rules:

1. The state $(\mu_t = \delta(p - p_t^0), p_t^0)$ is invariant if $p_t^0 \notin \mathcal{R}$. This law translates in measure space the fact that the jump process p_t does not move outside \mathcal{R}_t .
2. The process (μ_t, p_t^0) jumps from $(\mu_t = \delta(p - p_t^0), p_t^0)$ to $(\mu_t = I_{\mathcal{R}}(p), p_t^0)$ with rate $\frac{1}{\epsilon}$ when $p_t^0 \in \mathcal{R}_t$. This law translates in measure space the fact that the jump process p_t can jump to any point in \mathcal{R}_t with rate $1/(\epsilon\delta)$.
3. We define the variable $B\mathcal{R}_t := \nu_t - \text{sgn}(\dot{\nu}_t)\frac{\delta}{2}$, which corresponds to the boundary of \mathcal{R}_t opposite to the moving direction of ν_t . The process (μ_t, p_t^0) jumps from $(\mu_t = I_{\mathcal{R}}(p), p_t^0)$ to $(\mu_t = \delta(p - (B\mathcal{R}_t)), B\mathcal{R}_t)$ with rate $\frac{\dot{\nu}_t}{\delta}$. This corresponds to the exit from region \mathcal{R}_t . With the regularization (26) of the process ν_t , the jumping rate is perfectly defined.

The Markov process (ν_t, μ_t, p_t^0) described by the rules 1,2 and 3 is equivalent to the Markov jump process p_t which infinitesimal generator is given by (25). With the formalism of Young measures, the $\epsilon \rightarrow 0$ limit becomes straightforward: the process converges to the jump process defined by rules 1 and 3, and with the infinite rate limit for the second rule. This means that the process (μ_t, p_t^0) jumps instantaneously from $(\mu_t = \delta(p - p_t^0), p_t^0)$ to $(\mu_t = I_{\mathcal{R}}(p), p_t^0)$ as soon as $p_t^0 \in \mathcal{R}_t$. This gives a precise definition of the local diffusion model (23-24). We note however that the limit $\tau_c \rightarrow 0$ in this model leads to some troubles as the jump rate $\frac{\dot{\nu}_t}{\delta}$ becomes infinite. The question of the limit $\tau_c \rightarrow 0$ is a very interesting mathematical one, but it is out of the scope of this paper.

In this subsection, we have set up the mathematical framework. We have built two models: the first model is a Hamiltonian model (19) that depends on time and on frequencies with a slow stochastic evolution (21). The second model is completely stochastic, and can be thought of as the ‘‘averaging’’ of the first model. It is called the local diffusion model, and defined by equations (23-24). The great interest of the local diffusion model is that it is completely stochastic, and thus much simpler to study than the first model, which still keeps the complexity inherent to a chaotic dynamics.

We still did not explain on which conditions the local diffusion model should give relevant predictions for the stochastic Hamiltonian model, this is one crucial question that is answered in section 3.4. Section 3.4 presents the numerical simulations performed with the first model (19-21), with comparisons with the local diffusion model. We study in section 3.4 first exit times τ from a domain, both for the model (19-21) and for the local diffusion model. More precisely, we define the variable τ as the first time to reach $p = 0$ starting from $p = 10$. Our aim is then to compute numerically the probability distribution $\rho(\tau)$. In particular, we focus on the typical time τ^* where the probability distribution $\rho(\tau)$ reaches its maximal value, and on the dependance of the distribution on the noise amplitude σ .

Simulation	σ	$T_{max} \times \frac{\nu_1}{2\pi} \cdot 10^{-4}$
1	3.0	1.0
2	2.2	2.0
3	1.84	3.0
4	1.1	10.0
5	0.7	50.0

Table 2: Noise amplitudes and integration times of the five simulations in figure (8).

3.4 Comparison of the dynamics of the stochastic Hamiltonian model with the local diffusion model

3.4.1 Simulations of the Hamiltonian dynamics with stochastic frequencies

We now present the numerical results obtained with the stochastic Hamiltonian model defined by (19-21). The Hamiltonian (19) has the form $A(p) + B(q, t)$ with

$$A(p) := \frac{p^2}{2},$$

$$B(q, t) := \sum_{k=1}^4 \cos \left(q - \frac{1}{\epsilon} \int_0^t \nu_k(s) ds - \varphi_k \right).$$

We have thus used the symplectic integrator of order 4 $SBAB_3$ [37]. At each time step, we integrate the frequencies from equation (21) with a stochastic Euler algorithm. The parameter ϵ , the mean frequencies ν_k^* and the initial phases φ_k were fixed to their nominal values given in Table (1).

As we have explained at the end of Section 3.2, we are mainly interested in the first exit time τ defined as the first time to leave the region $p > 0$ starting from $p = 10$. We want to compute numerically its probability distribution function $\rho(\tau)$, and determine how it depends on the noise amplitude σ . To achieve this aim, we have performed a set of five numerical simulations using the values of σ given in Table 2. For each simulation, we ran 5000 trajectories all starting at the same point $(p, q) = (10, 0)$. Each trajectory is run with a different realization of the noise $W(t)$. The results of the simulations are the histograms displayed in figure (8). The histograms represent the distributions $\rho(\tau)$ for each simulation.

3.4.2 Simulations of the local diffusion model

The local diffusion model is given by equations (23-24). So far, we did not prescribe the values of the parameters δ_1, δ_2 corresponding to the extensions of the diffusion patches $\mathcal{R}_1, \mathcal{R}_2, \mathcal{R}_3$. δ_1 and δ_2 should correspond to the effective extension of the strongly chaotic regions of the stochastic Hamiltonian model. The parameters δ_1 and δ_2 could be estimated from the Chirikov criterion of resonance overlap. However, it is known [2] that the size of the chaotic regions is smaller than the theoretical predictions of the Chirikov criterion. This is confirmed here by the numerical simulations. To obtain a better agreement with the simulations, we prescribed the size of the diffusion patches with the following method.

To estimate the size of the chaotic region 1 (see figure 3), we ran a numerical simulation of Hamilton equations with the Hamiltonian (19), except that we kept the frequencies fixed to their reference values ν_i^* . We simulated 2000 trajectories with initial conditions $p = \nu_1^*$ and q equally distributed over the range $[0, 2\pi]$, over a time $T = 300 * \frac{2\pi}{\nu_1^*}$. The final coordinates are then distributed over the chaotic region 1, and only very few of them have exited region 1. Figure (7) shows a typical histogram of final momenta. We then define the boundaries of the chaotic region as the symmetric interval $[p_1, p_2]$ centered at $p = \frac{\nu_1^* + \nu_2^*}{2}$ in which 90% of the probability distribution is concentrated. Then, the empirical estimate of δ_1 is $\delta_1 \approx p_2 - p_1$.

Using the same method, we have estimated the extension $\delta_2, \delta_3, \delta_4$ of the chaotic regions corresponding to the resonances of second, third and fourth orders respectively. The regions are located around the values $p = 3.3$, $p = 6.6$ for the resonances of third order, and $p = 2.5$ and $p = 7.5$ for the resonances of fourth order. The values of $\{\delta_i\}_{i=1..4}$ are reported in table (3).

We ran $M = 1000$ simulations using for each a new realization of the stochastic process $\nu(t)$. For each of the realization $\nu(t)$, we could compute with (23) the density $g_\nu(p, t)$ of the probability to find the system at p at time t . At the beginning, the system is in $p = \nu_1^*$, which corresponds to the initial condition $g_\nu(p, 0) = \delta(p - \nu_1^*)$. We

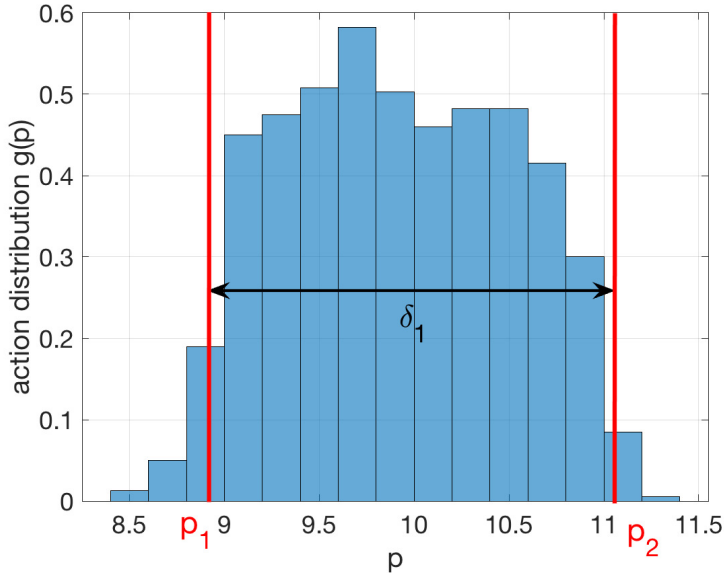


Figure 7: Histogram of the density in the chaotic region 1 after about 300 turnover times. The two red lines at p_1 and p_2 show the boundaries of the strongly chaotic region. The mixing region used in the local diffusion model is defined as the symmetric interval $[p_1, p_2]$ centered at $p = \frac{\nu_1^* + \nu_2^*}{2}$ in which 90% of the probability distribution is concentrated. Its extension is given by $\delta_1 = p_2 - p_1$.

want to compute the probability of first hitting time at $p = 0$. This means that we have to prescribe the boundary condition $g_\nu(p < 0, t) = 0$. In practice, this condition amounts to set $g_\nu(p, t) = 0$ for $p \in [\nu_4(t) - \delta_1/2, \nu_4(t) + \delta_1/2]$ because if the system enters in the diffusion patch \mathcal{R}_2 , it is immediately transported across the patch and reaches $p = 0$.

The complete probability distribution $g(p, t)$ is simply the average of $g_\nu(p, t)$ over the realizations of the stochastic process $\nu(t)$. Let $\{\nu^k(t)\}_{k=1..M}$ be the M realizations of $\nu(t)$, we have

$$g(p, t) = \frac{1}{M} \sum_{k=1}^M g_{\nu^k}(p, t).$$

Then the probability of first hitting times $\rho(\tau)$ is given by

$$\rho(\tau) = -\frac{d}{d\tau} \int_0^{+\infty} g(p, \tau) dp.$$

The simulations are performed with the set of parameters given in table (2). The results are displayed on the different graphs of figure (8) together with the histograms obtained by the direct Hamiltonian simulations. The curves show the results of $\rho(\tau)$ obtained with the simulations of the local diffusion model, whereas the histograms show the results for $\rho(\tau)$ obtained with the simulations of the stochastic Hamiltonian model. On the simulations 1, 2 and 3, we have only used the local diffusion model including the resonances up to second order. But on the simulations 4 and 5, there are two curves for $\rho(\tau)$: the lower one is the distribution $\rho(\tau)$ computed with the local diffusion model with resonances up to second order, but on simulation 4 and 5, we included the resonances up to fourth order in the local diffusion model. The results are displayed by the upper curves in simulations 4 and 5.

3.5 Discussion

The different simulations in figure (8) aim at showing which phenomenon governs the transport in phase space in the stochastic Hamiltonian model (19-21), and how the transport depends on the parameters of the model.

One trivial but crucial conclusion of our numerical study is that the transport in a stochastic Hamiltonian model is very different from the transport with the same Hamiltonian (19) without stochastic variations of the frequencies. If the frequencies are fixed, the trajectories starting at $p = \nu_1^*$ are just spread across the first mixing region, and

resonances	extension of the chaotic region	numerical estimation of $p_2 - p_1$
first order	δ_1	2.25
second order	δ_2	0.50
third order	δ_3	0.28
fourth order	δ_4	0.09

Table 3: Width of the diffusion patches of the local diffusion model.

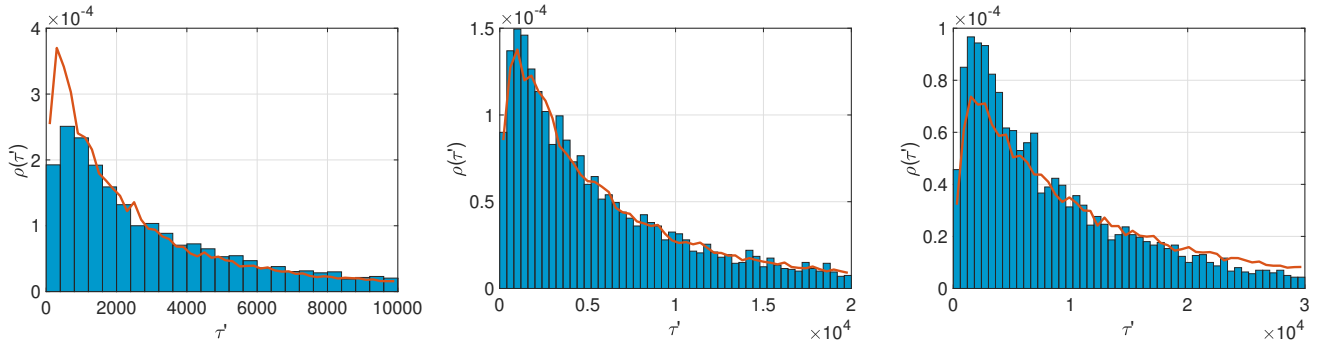


Figure 8: First exit time distributions $\rho(\tau)$ for three simulations with $\sigma = 3.0$ (left), $\sigma = 2.2$ (middle) and $\sigma = 1.84$ (right). We display the distributions in terms of the non-dimensional time $\tau' := \tau \times \frac{\nu_1}{2\pi}$. The histograms display the results of the simulations with the Hamiltonian (19). The curves show the results of the corresponding local diffusion model including resonances up to second order.

none of them reaches the value $p = 0$ within the time T_{max} . Transport with stochastic frequencies is thus a new mechanism that completely overcomes chaotic diffusion in deterministic chaotic Hamiltonian dynamics.

The qualitative shape of the distributions of first hitting times $\rho(\tau)$ displayed in figure (8) is typical of a distribution of first exit times from a domain in a stochastic system. The probability distribution has a maximum ρ^* reached at τ^* , that can be considered as the typical time for the exit event to occur. For times smaller than τ^* , the probability distribution goes rapidly to zero. It is thus very rare for the system to reach $p = 0$ in a time much smaller than the typical time τ^* , because it corresponds to exceptionally large and fast random fluctuations of the stochastic frequencies $\{\nu_i\}$. For times larger than the typical time τ^* , the probability distribution also goes to zero because it is also a rare event, called ‘‘persistence’’, that the system does not leave the domain $p > 0$ for a long time.

The order of magnitude of τ^* depends on the noise amplitude σ acting on the frequencies. For $\sigma = 3.0$, it is of the order of $10^3 * \frac{2\pi}{\nu_1^*}$, whereas for $\sigma = 0.7$, it is two orders of magnitude larger, of the order of $10^5 * \frac{2\pi}{\nu_1^*}$. We have checked numerically that the typical exit time τ^* does not depend on ϵ in the limit $\epsilon \rightarrow 0$. This fact shows that the transport mechanism has a well defined limit when $\epsilon \rightarrow 0$, and confirm the relevance of the local diffusion model.

The local diffusion model presented in Section 3.2 can be seen as the averaged dynamics of the stochastic Hamiltonian model, for which transport outside of the principal chaotic regions has been neglected. This is reflected in the local diffusion model by the fact that the diffusion coefficient is zero outside the diffusion patches \mathcal{R}_i . Therefore, the local diffusion model only takes into account transport by migration with the chaotic regions. If the transport of this type is dominant, it is natural to expect that the local diffusion model reproduces well the results of the stochastic Hamiltonian model. If, on contrary, transport is mainly due to the mechanism of noise driven transport in regular regions, then the exit rate at $p = 0$ predicted by the local diffusion model is much slower than the real transport of the Hamiltonian dynamics with stochastic parameters.

On figure (8), it can be seen that the local diffusion model is able to capture quite well the probability distribution of first exit times $\rho(\tau)$. For the three simulations with $\sigma = 3.0/2.2/1.84$, the local diffusion model including resonances up to second order gives excellent results. It reproduce qualitatively and quantitatively the histogram of $\rho(\tau)$, with the same location τ^* of the maximal value, and reproduces the decrease of the distribution $\rho(\tau)$ for long times. For the two simulations with $\sigma = 1.1/0.7$ the local diffusion model of second order predicts a transport rate which is much smaller than the real transport. In particular for $\sigma = 0.7$, even the qualitative shape of $\rho(\tau)$ for the Hamiltonian model is not reproduced, the typical time τ^* is by far overestimated. This means that for σ values below 1.84, transport through resonances of order higher than two can no longer be neglected. The local diffusion model including resonances up to fourth order is able to reproduce qualitatively the distribution of exit

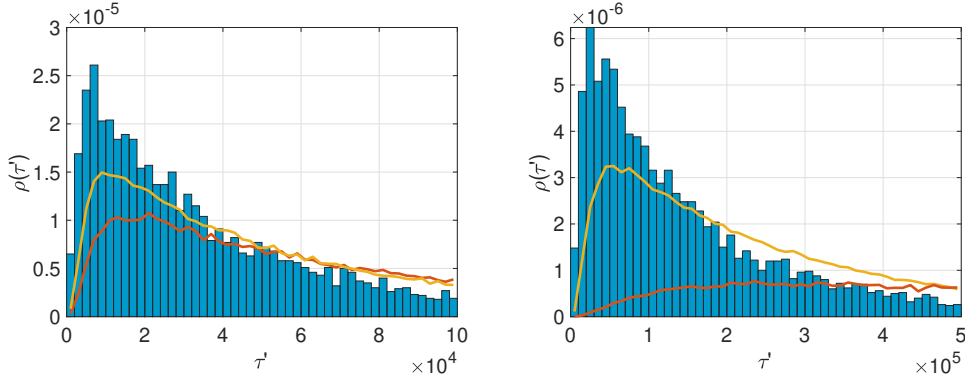


Figure 9: First exit time distributions $\rho(\tau)$ for two simulations with $\sigma = 1.1$ (left) and $\sigma = 0.7$ (right). We display the distributions in terms of the non-dimensional time $\tau' := \tau \times \frac{\nu_1}{2\pi}$. The histograms display the results of the simulations with the Hamiltonian (19). The lower curves (red) show the results of the corresponding local diffusion model including resonances up to second order, and the upper curves (yellow) show the results of the local diffusion model including resonances up to fourth order.

times $\rho(\tau)$, and gives also a good order of magnitude of the value of $\rho(\tau)$. This is illustrated by the upper curves for the simulations 4 and 5 on figure (8). For values of σ below 0.7, the local diffusion model is no longer able to reproduce transport in phase space, even with resonances up to fourth order. This comes from the fact that the overlap of two neighboring chaotic regions becomes very rare when σ decreases, and thus the mechanism of noise driven transport in the regular regions overcomes the first mechanism.

The relevance of the local diffusion model to predict transport depends on the balance between the amplitude σ of frequencies fluctuations and the distance to cross between two neighboring diffusion regions. For example, in the local diffusion model of order two, the initial distance between two neighboring diffusion patches is

$$\text{Dist}_{\mathcal{R}_1 \rightarrow \mathcal{R}_3} := \left(\frac{\nu_1^* + \nu_2^*}{2} - \frac{\delta_1}{2} \right) - \left(\frac{\nu_1^* + \nu_4^*}{2} + \frac{\delta_2}{2} \right) \approx 3.575.$$

The sum of the variances of the fluctuations of the diffusion patches \mathcal{R}_1 and \mathcal{R}_3 gives the typical amplitude of the fluctuations of the mixing regions

$$\sqrt{V_{\mathcal{R}_1} + V_{\mathcal{R}_3}} = \left(1 + \frac{1}{\sqrt{2}} \right) \sigma,$$

where $V_{\mathcal{R}_i}$ is the variance of fluctuations of region i . Therefore, the efficiency of the transport through migration of the mixing regions depends on whether the parameter

$$\Delta := \frac{\text{Dist}_{\mathcal{R}_1 \rightarrow \mathcal{R}_3}}{\sqrt{V_{\mathcal{R}_1} + V_{\mathcal{R}_3}}} \simeq \frac{2.1}{\sigma}$$

is large or small compared to one.

This means that for the three simulations with $\sigma = 3.0/2.2/1.84$, the initial distance to cross between two diffusion patches is larger or of same order as the amplitude of the frequency fluctuations. The jump between one diffusion patch to another is thus possible with “typical” fluctuations of the frequencies. Transport does not require an exceptionally large fluctuation. But this is no longer the case for $\sigma = 1.1/0.7$. Frequency fluctuations are too small to pass directly from the mixing region surrounding the first order resonances to the mixing region surrounding the second order resonances (or equivalently, from \mathcal{R}_1 to \mathcal{R}_3), and transport is due to higher order resonances. For example, in the local diffusion model of fourth order, the initial distance to cross to jump from the diffusion patch \mathcal{R}_1 to the next patch \mathcal{R}_3 is $\text{Dist}_{\mathcal{R}_1 \rightarrow \mathcal{R}_3} = \left(\frac{\nu_1^* + \nu_2^*}{2} - \frac{\delta_1}{2} \right) - \left(\frac{3\nu_1^* + \nu_4^*}{2} + \frac{\delta_4}{2} \right) \approx 1.28$. On the other hand, the combined fluctuations of the two patches have a variance of $\sqrt{V_{\mathcal{R}_1} + V_{\mathcal{R}_3}} = \left(1 + \frac{\sqrt{10}}{4} \right) \sigma$. Thus the parameter Δ is of the order of $\Delta \simeq \frac{1.28}{1 + \sqrt{10}/4} \frac{1}{\sigma} \simeq \frac{0.71}{\sigma}$. This argument explains why the local diffusion model up to order four is able to predict the transport for values of σ of the order of 0.7, but fails for lower values of σ .

In the present section, we have shown how a system that satisfies a Hamiltonian dynamics with stochastic frequencies can be transported slowly through phase space by the slow displacement of the chaotic regions. We have shown that this kind of transport can be reproduced qualitatively and quantitatively by a Markov model, the local diffusion model. The local diffusion model gives a representation of the strongly chaotic regions created by resonance overlap by diffusion patches with infinite diffusion coefficient. The relevance of this Markov model to predict transport rates in the stochastic Hamiltonian model mainly depends on the amplitude of the frequency stochastic variations. We have shown that for decreasing amplitudes of the variations, the local diffusion model should take into account resonances of higher and higher orders. In this section, we have presented a model including resonances up to order four. But one cannot expect the local diffusion model to be valid for all range of the amplitude fluctuations σ , even if we include resonances up to higher orders. The reason for that is that transport is also due to noise driven transport in the regular regions, away from the resonances. If the amplitude of the fluctuations is too small, then transport is mainly due to noise driven transport in the regular regions. We have shown that transport is mainly due to migration with the chaotic regions if the typical fluctuations of the frequencies are similar to the distance in phase space between two neighboring chaotic regions.

We have performed an other numerical simulation where the stochastic process for the variations of ν is a jump process with exponential distribution of the jumps, and we found that the results are in agreement with the general picture we give in this section. This suggests that the transport mechanism described in this article is robust to a change in the stochastic process for the evolution of the external parameter.

4 Conclusion

We have studied time dependent Hamiltonian systems with one degree of freedom, for which the Hamiltonian depends on an additional slow stochastic parameter. The slowly varying parameter introduces a timescale separation in the system, which allows us to use the theory of averaging to describe the long term evolution of the system. When the fast Hamiltonian dynamics is integrable, it has been shown that the slow evolution can be described by a diffusion process of the action variable. This first part of our work is mostly an extension of the theory of adiabatic invariants to the stochastic case. Because of the irregularity of the stochastic process, adiabatic invariants are not conserved in the limit of a large timescale separation, unlike in the classical theory. This gives a new mechanism of transport that we call "noise driven transport in regular regions".

More interesting for practical applications is the case where the fast Hamiltonian dynamics is chaotic. We have shown that transport in phase space comes from the slow displacement of chaotic regions, and is equivalent, for some ranges of the parameters, to a Markov process called the local diffusion model. We have shown numerically that the local diffusion model give quantitative results in agreement with the full simulations of the Hamiltonian dynamics with stochastic parameters.

This work can be seen as a pioneer work on a new class of dynamical systems, Hamiltonian dynamical systems with slowly changing phase space structure. By no mean does this work intend to be exhaustive on the subject. In particular, our work leaves many open questions. First, it has been shown in section 2 that the mechanism of noise-driven transport comes from the strong irregularity of the stochastic process. One could wonder what happens when the stochastic process is smooth, with a finite correlation time. How does transport depend on this new timescale? And how does the transition happens to the white noise limit presented in our work? Also, while our theory do not consider separatrix crossing for integrable dynamics, it is known that separatrix crossing occurs in numerous physical situations and an extension of our theory would be interesting in this case. In section 3, we focused on the mechanism of "transport by slow migration with the chaotic regions". A full description of transport in the chaotic case presented in section 3 should also include extension of the chaotic regions, that was neglected in the present work.

The reduction of the dynamics to a Markov process opens the possibility to use large deviation theory to compute the probability of rare events in the dynamical system, for example the probability of an exceptionally fast exit out of a domain. Simplified Hamiltonian models with few degrees of freedom and a stochastic parameter can be used as preliminary works to find qualitative behaviors and order of magnitudes before resorting to involved numerical simulations. It is hoped that our work will find interesting applications in celestial mechanics and other domains of physics.

Acknowledgement

We thank Cristel Chandre for his help in the preliminary stage of this work. We also thank Jacques Laskar whose work on the chaotic obliquity of planets has been the main motivation of the present work. The research leading to these results has received funding from the European Research Council under the European Union's seventh Framework Program (FP7/2007-2013 Grant Agreement No. 616811).

References

- [1] GM Zaslavsky. Chaos, fractional kinetics, and anomalous transport. *Physics reports*, 371(6):461–580, 2002.
- [2] AJ Lichtenberg and MA Lieberman. *Regular and stochastic motion*, volume 38. Springer Science & Business Media, 2013.
- [3] S Wiggins. *Chaotic transport in dynamical systems*, volume 2. Springer Science & Business Media, 2013.
- [4] JD Meiss. Thirty years of turnstiles and transport. *Chaos: An Interdisciplinary Journal of Nonlinear Science*, 25(9):097602, 2015.
- [5] Y Elskens and DF Escande. *Microscopic dynamics of plasmas and chaos*. CRC Press, 2002.
- [6] DF Escande. From thermonuclear fusion to hamiltonian chaos. *The European Physical Journal H*, 43(4-5):397–420, 2018.
- [7] F Moss and PVE McClintock. *Noise in Nonlinear Dynamical Systems: Theory of noise induced processes in special applications*. Cambridge University Press, 1989.
- [8] AB Rechester and RB White. Calculation of turbulent diffusion for the chirikov-taylor model. *Physical Review Letters*, 44(24):1586, 1980.
- [9] AB Rechester, MN Rosenbluth, and RB White. Fourier-space paths applied to the calculation of diffusion for the chirikov-taylor model. *Physical Review A*, 23(5):2664, 1981.
- [10] CFF Karney, AB Rechester, and RB White. Effect of noise on the standard mapping. *Physica D: Nonlinear Phenomena*, 4(3):425–438, 1982.
- [11] MA Lieberman and AJ Lichtenberg. Stochastic and adiabatic behavior of particles accelerated by periodic forces. *Physical Review A*, 5(4):1852, 1972.
- [12] M Freidlin and AD Wentzell. Random perturbations. In *Random Perturbations of Dynamical Systems*, pages 15–43. Springer, 1984.
- [13] M Freidlin and A Wentzell. Some recent results on averaging principle. *Topics in Stochastic Analysis and Nonparametric Estimation*, pages 1–19, 2008.
- [14] A Bazzani, S Siboni, and G Turchetti. Action diffusion for symplectic maps with a noisy linear frequency. *Journal of Physics A: Mathematical and General*, 30(1):27, 1997.
- [15] A Bazzani and L Beccaceci. Diffusion in hamiltonian systems driven by harmonic noise. *Journal of Physics A: Mathematical and General*, 31(28):5843, 1998.
- [16] D. V. Makarov and M. Yu. Uleysky. Giant acceleration in slow-fast space-periodic hamiltonian systems. *Phys. Rev. E*, 75:065201, Jun 2007.
- [17] D. V. Makarov, E. V. Sosedko, and M. Yu. Uleysky. Frequency-modulated ratchet with autoresonance. *The European Physical Journal B*, 73(4):571–579, Feb 2010.
- [18] M. Yu. Uleysky, E. V. Sosedko, and D. V. Makarov. Autoresonant cooling of particles in spatially periodic potentials. *Technical Physics Letters*, 36(12):1082–1084, Dec 2010.
- [19] DV Makarov, M Yu Uleysky, and SV Prants. Control of atomic transport using autoresonance. In *Chaos, Complexity and Transport*, pages 24–32. World Scientific, 2012.

- [20] N Brännström and V Gelfreich. Drift of slow variables in slow-fast hamiltonian systems. *Physica D: Nonlinear Phenomena*, 237(22):2913–2921, 2008.
- [21] Vassili Gelfreich and Dmitry Turaev. Unbounded energy growth in hamiltonian systems with a slowly varying parameter. *Communications in Mathematical Physics*, 283(3):769, 2008.
- [22] RM Kulsrud. Adiabatic invariant of the harmonic oscillator. *Physical Review*, 106(2):205, 1957.
- [23] CS Gardner. Adiabatic invariants of periodic classical systems. *Physical Review*, 115(4):791, 1959.
- [24] AI Neishtadt. On the change in the adiabatic invariant on crossing a separatrix in systems with two degrees of freedom. *Journal of Applied Mathematics and Mechanics*, 51(5):586–592, 1987.
- [25] JL Tennyson, John R Cary, and DF Escande. Change of the adiabatic invariant due to separatrix crossing. *Physical review letters*, 56(20):2117, 1986.
- [26] J Henrard. Capture into resonance: an extension of the use of adiabatic invariants. *Celestial Mechanics and Dynamical Astronomy*, 27(1):3–22, 1982.
- [27] J Laskar. A numerical experiment on the chaotic behaviour of the solar system. *Nature*, 338(6212):237–238, mar 1989.
- [28] J Laskar. The chaotic motion of the solar system: a numerical estimate of the size of the chaotic zones. *Icarus*, 88(2):266–291, 1990.
- [29] J Laskar, P Robutel, F Joutel, M Gastineau, ACM Correia, and B Levrard. A long-term numerical solution for the insolation quantities of the earth. *Astronomy & Astrophysics*, 428(1):261–285, 2004.
- [30] E Woillez. *Stochastic description of rare events for complex dynamics in the solar system*. PhD thesis, ENS de Lyon, 2018.
- [31] A Bazzani, C Frye, M Giovannozzi, and C Hernalsteens. Analysis of adiabatic trapping for quasi-integrable area-preserving maps. *Physical Review E*, 89(4):042915, 2014.
- [32] CW Gardiner. *Stochastic methods*. Springer-Verlag, Berlin–Heidelberg–New York–Tokyo, 1985.
- [33] Kirone Mallick and Philippe Marcq. Anomalous diffusion in nonlinear oscillators with multiplicative noise. *Physical Review E*, 66(4):041113, 2002.
- [34] F Bouchet, T Grafke, T Tangarife, and E Vanden-Eijnden. Large deviations in fast–slow systems. *Journal of Statistical Physics*, 162(4):793–812, 2016.
- [35] M Freidlin. The averaging principle and theorems on large deviations. *Russian mathematical surveys*, 33(5):117, 1978.
- [36] Y Kifer. Averaging principle for fully coupled dynamical systems and large deviations. *Ergodic Theory and Dynamical Systems*, 24(03):847–871, 2004.
- [37] H Yoshida. Construction of higher order symplectic integrators. *Physics letters A*, 150(5-7):262–268, 1990.

A Averaging in slow-fast system when the slow dynamics is a diffusion process

In the present section, we explain how to average the slow-fast system (10) to obtain closed stochastic differential equations for the variables ν and P . The difficult step comes from the average of the stochastic term

$$d\xi := \sigma(Q, P, \nu)dW,$$

where σ is the vector

$$\sigma := \begin{pmatrix} b(\nu) \\ b(\nu) \frac{\partial H_1}{\partial Q}(Q, P, \nu) \end{pmatrix},$$

and W is a one-dimensional Wiener process.

A variation $\Delta\xi$ over a given fixed time interval Δt is given by

$$\Delta\xi = \int_0^{\Delta t} \sigma(Q(t'), P(t'), \nu(t')) dW(t'). \quad (27)$$

According to the first equation of (10), Q is a fast variable, which means that it is in fact a function of $\frac{t}{\epsilon}$, with $\epsilon \ll 1$. If we consider a time interval Δt small enough, the increment of the functions $\nu(t)$ and $P(t)$ during Δt can be considered as constant in (27) to leading order. This assumption will turn out to be self-consistent. Accordingly, we can write (27) as

$$\Delta\xi = \int_0^{\Delta t} \sigma(Q(t'/\epsilon), P, \nu) dW(t'). \quad (28)$$

Then, using the property of self-similarity for the Wiener process, namely that $W(\epsilon t') = \sqrt{\epsilon}W(t')$, the increment (28) becomes

$$\Delta\xi = \sqrt{\epsilon} \int_0^{\Delta t/\epsilon} \sigma(Q(t'), P, \nu) dW(t'). \quad (29)$$

The stochastic integral in (29) has to be understood as a sum of independent Gaussian random variables (see [32]). Partitioning the interval $\Delta t/\epsilon$ in N small intervals $[t_i, t_{i+1}]$, the stochastic integral (29) is the large N limit of the sum

$$\Delta\xi = \lim_{N \rightarrow \infty} \sqrt{\epsilon} \sum_{i=1}^N \sigma(Q(t_i), P, \nu) dW_i, \quad (30)$$

where all the variables dW_i are independent Gaussian random variables with zero mean and variance $\frac{\Delta t}{\epsilon N}$. Now, the key property is that a sum of independent Gaussian random variables is a random variable. To find the limit in (30), one just has to compute the variance of the sum. We get

$$\begin{aligned} \langle (\Delta\xi)^2 \rangle &= \lim_{N \rightarrow \infty} \epsilon \sum_{i,j=1}^N \sigma(Q(t_i), P, \nu) \sigma^T(Q(t_j), P, \nu) \langle dW_i dW_j \rangle, \\ &= \lim_{N \rightarrow \infty} \frac{\Delta t}{N} \sum_{i=1}^N \sigma \sigma^T(Q(t_i), P, \nu), \end{aligned}$$

where the last equality has been obtained using that $\langle dW_i dW_i \rangle = \frac{\Delta t}{\epsilon N}$, and $\langle dW_i dW_j \rangle = 0$ if $i \neq j$. The final step is to notice that the average

$$\frac{1}{N} \sum_{i=1}^N \sigma \sigma^T(Q(t_i), P, \nu)$$

is done over the time interval $\frac{\Delta t}{\epsilon}$, with $\epsilon \ll 1$. Over this timescale, the time average corresponds to the average over the invariant measure of the process $Q(t)$. The final result is

$$\langle (\Delta\xi)^2 \rangle = \Delta t \langle \sigma \sigma^T(Q, P, \nu) \rangle_Q.$$

This justifies the computation of the average in (11), and the result in (12).

It is important to bear in mind that this result is obtained from the property that the white noise has a vanishing correlation time. This hypothesis is implicit in the change of timescale in (29). The above result would not be true if we had considered, instead of a diffusion process with white noise, a fast process with a finite correlation time τ_c of the order of ϵ . The mechanism of "noise driven transport in regular regions" that we describe in section 2 would not be the same if the noise in the equation for ν would have a correlation time of the same order as the typical time for the variations of Q .

B Canonical change of variables and existence of a function H_1 such that $\frac{\partial P}{\partial \nu} = -\frac{\partial H_1}{\partial Q}$ and $\frac{\partial Q}{\partial \nu} = \frac{\partial H_1}{\partial P}$

Let (p, q) be the canonical variables of the Hamiltonian $H(p, q, \nu)$ where is ν an external parameter of the Hamiltonian. We assume that for a given value of ν , the Hamiltonian H is integrable, which means that for any ν there

exist canonical variables $(P(p, q, \nu), Q(p, q, \nu))$ such that $H(p, q, \nu) = \tilde{H}(P, \nu)$, and \tilde{H} does not depend on Q . By definition, a change of variable is canonical one whenever the differential two form is conserved: $dP \wedge dQ = dp \wedge dq$, or equivalently the Poisson bracket $\{P, Q\}_{p,q} = 1$, where $\{f, g\}_{p,q} = \frac{\partial f}{\partial p} \frac{\partial g}{\partial q} - \frac{\partial f}{\partial q} \frac{\partial g}{\partial p}$. The aim of this section is to prove that there exists a function $H_1(P, Q, \nu)$ such that $\frac{\partial P}{\partial \nu}(p, q, \nu) = -\frac{\partial H_1}{\partial Q}(Q(p, q, \nu), P(p, q, \nu), \nu)$ and $\frac{\partial Q}{\partial \nu}(p, q, \nu) = \frac{\partial H_1}{\partial P}(Q(p, q, \nu), P(p, q, \nu), \nu)$ (relation (9) in the main text).

In order to prove this result, we extend the phase space by introducing V the canonical momentum associated to ν . We consider an extended Hamiltonian with two degrees of freedom

$$H'(p, q, V, \nu) := H(p, q, \nu) + V.$$

This amounts to saying that ν has a dynamics, with $\dot{\nu} = \frac{\partial H'}{\partial V} = 1$. We will show that we can find a new momentum V' such that the change of variables $(p, q, V, \nu) \rightarrow (P, Q, V', \nu')$ is canonical, where $(P(p, q, \nu), Q(p, q, \nu))$ are the canonical variable defined above for any fixed ν , and the new variable ν' is such that $\nu' := \nu$. A change of variable is canonical if and only if the differential two-form is conserved, which can be expressed as

$$dP \wedge dQ + dV' \wedge d\nu' = dp \wedge dq + dV \wedge d\nu. \quad (31)$$

Then we express explicitly the differentials dP and dQ as

$$\begin{aligned} dP &= \frac{\partial P}{\partial p} dp + \frac{\partial P}{\partial q} dq + \frac{\partial P}{\partial \nu} d\nu, \\ dQ &= \frac{\partial Q}{\partial p} dp + \frac{\partial Q}{\partial q} dq + \frac{\partial Q}{\partial \nu} d\nu, \end{aligned}$$

and we use these relations in (31) to obtain

$$\{P, Q\}_{p,q} dp \wedge dq + \{P, Q\}_{p,\nu} dp \wedge d\nu + \{P, Q\}_{q,\nu} dq \wedge d\nu + dV' \wedge d\nu' = dp \wedge dq + dV \wedge d\nu. \quad (32)$$

In the first wedge product, the Poisson bracket satisfies $\{P, Q\}_{p,q} = 1$, thus (32) becomes

$$\{P, Q\}_{p,\nu} dp \wedge d\nu + \{P, Q\}_{q,\nu} dq \wedge d\nu + dV' \wedge d\nu' = dV \wedge d\nu. \quad (33)$$

We now use that $\nu' = \nu$. We look for a function $H_1(Q, P, \nu)$ such that the canonical momentum V' has the form $V' = V - H_1$. Using the latter transformation, the equality (33) becomes

$$\left(\{P, Q\}_{p,\nu} dp + \{P, Q\}_{q,\nu} dq - dH_1 \right) \wedge d\nu = 0.$$

This means that we can find a canonical change of variables iff

$$\{P, Q\}_{p,\nu} dp + \{P, Q\}_{q,\nu} dq = dH_1,$$

that is, iff the differential form $\{P, Q\}_{p,\nu} dp + \{P, Q\}_{q,\nu} dq$ is exact. Following a theorem of Riemann, a form is exact on a simple connected domain if and only if it is closed. The Poisson brackets should thus satisfy

$$\frac{\partial}{\partial q} \{P, Q\}_{p,\nu} = \frac{\partial}{\partial p} \{P, Q\}_{q,\nu}. \quad (34)$$

With some simple manipulations, we can write equality (34) as

$$\frac{\partial}{\partial \nu} \{P, Q\}_{p,q} = 0,$$

which is satisfied thanks to the relation $\{P, Q\}_{p,q} = 1$.

We have just proven the existence of H_1 . The new Hamiltonian can be expressed in terms of the variables (P, Q, V', ν') as

$$H(p, q, V, \nu) = \tilde{H}(P, \nu') + H_1(P, Q, \nu') + V'.$$

Therefore, the time evolution of the canonical variables is

$$\begin{aligned} \frac{dP}{dt} &= -\frac{\partial H_1}{\partial Q}, \\ \frac{dQ}{dt} &= \frac{\partial \tilde{H}}{\partial P} + \frac{\partial H_1}{\partial P}. \end{aligned} \quad (35)$$

But on the other hand, we know that the time evolution satisfies

$$\begin{aligned}\frac{dP}{dt} &= \frac{\partial P}{\partial \nu} \dot{\nu}, \\ \frac{dQ}{dt} &= \frac{\partial \tilde{H}}{\partial P} + \frac{\partial Q}{\partial \nu} \dot{\nu}.\end{aligned}\tag{36}$$

The identification of the equalities (35) and (36), with $\dot{\nu} = 1$, gives the desired result.